Geochemistry Geophysics Geosystems G3

Article
Volume 14, Number 8
22 August 2013
doi: 10.1002/ggge.20217
ISSN: 1525-2027

Published by AGU and the Geochemical Society

Tropical cyclone wind speed constraints from resultant storm surge deposition: A 2500 year reconstruction of hurricane activity from St. Marks, FL

Christine M. Brandon and Jonathan D. Woodruff
Department of Geosciences, 611 N. Pleasant St., 233 Morrill Science Center, University of Massachusetts Amherst, Amherst, Massachusetts, 01003, USA (cbrandon@geo.umass.edu)

D. Phil Lane and Jeffrey P. Donnelly
Department of Geology and Geophysics, Woods Hole Oceanographic Institution, Woods Hole, Massachusetts, USA

[1] Recent work suggests that the patterns of intense (≥category 3 on the Saffir-Simpson scale) hurricane strikes over the last few millennia might differ from that of overall hurricane activity during this period. Prior studies typically rely on assigning a threshold storm intensity required to produce a sedimentological overwash signal at a particular coastal site based on historical analogs. Here, we improve on this approach by presenting a new inverse-model technique that constrains the most likely wind speeds required to transport the maximum grain size within resultant storm deposits. As a case study, the technique is applied to event layers observed in sediments collected from a coastal sinkhole in northwestern Florida. We find that (1) simulated wind speeds for modern deposits are consistent with the intensities for historical hurricanes affecting the site, (2) all deposits throughout the ~2500 year record are capable of being produced by hurricanes, and (3) a period of increased intense hurricane frequency is observed between ~1700 and ~600 years B.P. and decreased intense storm frequency is observed from ~2500 to ~1700 and ~600 years B.P. to the present. This is consistent with prior reconstructions from nearby sites. Changes in the frequency of intense hurricane strikes may be related to the degree of penetration of the Loop Current in the Gulf of Mexico.

Components: 11,207 words, 8 figures, 1 table.

Keywords: tropical cyclones; paleotempestology; paleoclimate; holocene; inverse-modeling; sedimentology.

Index Terms: 4564 Tsunamis and storm surges: Oceanography: Physical; 4558 Sediment transport: Oceanography: Physical; 1862 Sediment transport: Hydrology; 4304 Oceanic: Natural Hazards; 4302 Geological: Natural Hazards; 1641 Sea level change: Global Change.

Received 29 April 2013; **Revised** 1 July 2013; **Accepted** 1 July 2013; **Published** 22 August 2013.

Brandon, C. M., J. D. Woodruff, D. Phil Lane, and J. P. Donnelly (2013), Tropical cyclone wind speed constraints from resultant storm surge deposition: A 2500 year reconstruction of hurricane activity from St. Marks, FL, *Geochem. Geophys. Geosyst.*, *14*, 2993–3008, doi:10.1002/ggge.20217.

1. Introduction

[2] The number of studies pertaining to tropical cyclone (called "hurricane" in the North Atlantic Ocean) proxies preserved within the geologic record have increased rapidly over the last two decades. This relatively new field of paleotempestology is fueled by a growing appreciation for the application of these records in hurricane risk assessments [e.g., *Murnane et al*., 2000; *Nott*, 2004; *Elsner et al*., 2008] and in identifying past long-term shifts in hurricane climatology [e.g., *Mann et al*., 2009]. Many studies have been conducted to extend the hurricane strike record at various locations in the western North Atlantic by identifying deposits in the sediment record left by hurricane storm surges and wave run-up [*Liu and Fearn*, 1993, 2000; *Donnelly et al*., 2001a, 2001b; *Donnelly and Woodruff*, 2007; *Scileppi and Donnelly*, 2007; *Woodruff et al*., 2008b; *Boldt et al*., 2010; *Wallace and Anderson*, 2010; *Lane et al*., 2011]. Other proxies of paleo-hurricane activity include extreme-precipitation events associated with hurricanes using $\delta^{18}O$ records from speleothems [*Malmquist*, 1997; *Frappier et al*., 2007] and tree rings [*Miller et al*., 2006]; increased river run-off and its effect on the growth and luminescence of coral [*Lough*, 2007; *Nyberg et al*., 2007]; and coarse deposits interpreted as intense terrestrial flooding events [*Noren et al*., 2002; *Besonen et al*., 2008]. Together, these proxy records provide an increasing body of knowledge of paleo-hurricane history in the Gulf of Mexico and the Northwestern Atlantic Ocean.

[3] In prior work, past geologic reconstructions of tropical cyclone activity have mainly documented changes in the reoccurrence rates of hurricanes above some assumed threshold based on modern calibration. In addition to documenting event occurrences, grain size distributions within hurricane deposits also provide information on the intensity of flooding by past hurricane strikes [*Woodruff et al*., 2008b]. However, the overall flooding magnitude at a location is influenced by factors in addition to the storm intensity. For example, a category 1 storm that directly hits a site could produce a similar storm surge as a category 5 storm making landfall much farther away. Accurate methods for back-calculating hurricane wind speed from resultant deposits must therefore account for these uncertainties.

[4] In this study, we present a new ~2500 year reconstruction of hurricane occurrences based on event-deposits preserved within a coastal sinkhole in western Florida. We use a series of nested modeling techniques to develop relationships between storm intensity and the maximum grain size that the resulting flows can carry to the site (i.e., transport competence). The obtained wind speed/transport competence relationship is then used to constrain the likely wind speed required to transport the maximum grain size observed within each individual deposit and to provide a reconstruction of hurricane intensity at the site.

2. Regional Setting and Site Description

[5] Spring Creek Pond (SCP), the coastal sinkhole considered in this study, is located ~2.8 km inland from Apalachee Bay and is part of the Big Bend region of Florida's northwest coast (Figure 1a). The pond is nearly circular and has a diameter of ~120 m. While much of the pond has an average depth of ~1 m, the sinkhole itself is ~15 m deep and has a diameter of ~60 m (darker portion of water in Figure 1b). The elevation of this freshwater pond is ~2.75 m above mean sea level. Between the pond and the coast the relatively undeveloped terrain is lightly forested and gradually slopes seaward.

[6] Hurricanes commonly affect Apalachee Bay, with the eye of a hurricane currently passing within 93 km (50 nautical miles) of the site on average once every 13 years (NOAA/National Weather Service, available from http://www. nhc.noaa.gov/climo/#returns). The bay is 400 km^2 in area, with an average submerged depth of 3 m [*USEPA*, 1999; *Lane et al*., 2011], a topographic and bathymetric across-shore gradient of 1:5000 [*Hine et al*., 1988], and an astronomical tidal range of 0.7 m [*Lane et al*., 2011; NOAA, available from http://tidesandcurrents.noaa.gov]. Hurricane-induced flooding within the Bay is particularly destructive because its concave coastline focuses storm surge, the shallow bathymetric depth allows a larger surge to form, and the shallow topographic slope allows these surges to inundate great distances inland [*Jelesnianski et al*., 1992; *Lane et al*., 2011].

[7] The underlying bedrock of the coast and coastal shelf of Apalachee Bay (and a large portion of Florida) is Eocene/Oligocene age limestone, emplaced when the area was submerged beneath a shallow sea [*Hine et al*., 1988; *Wright et al*., 2005]. Today's karst landscape is the result of dissolution of the limestone bedrock over millions

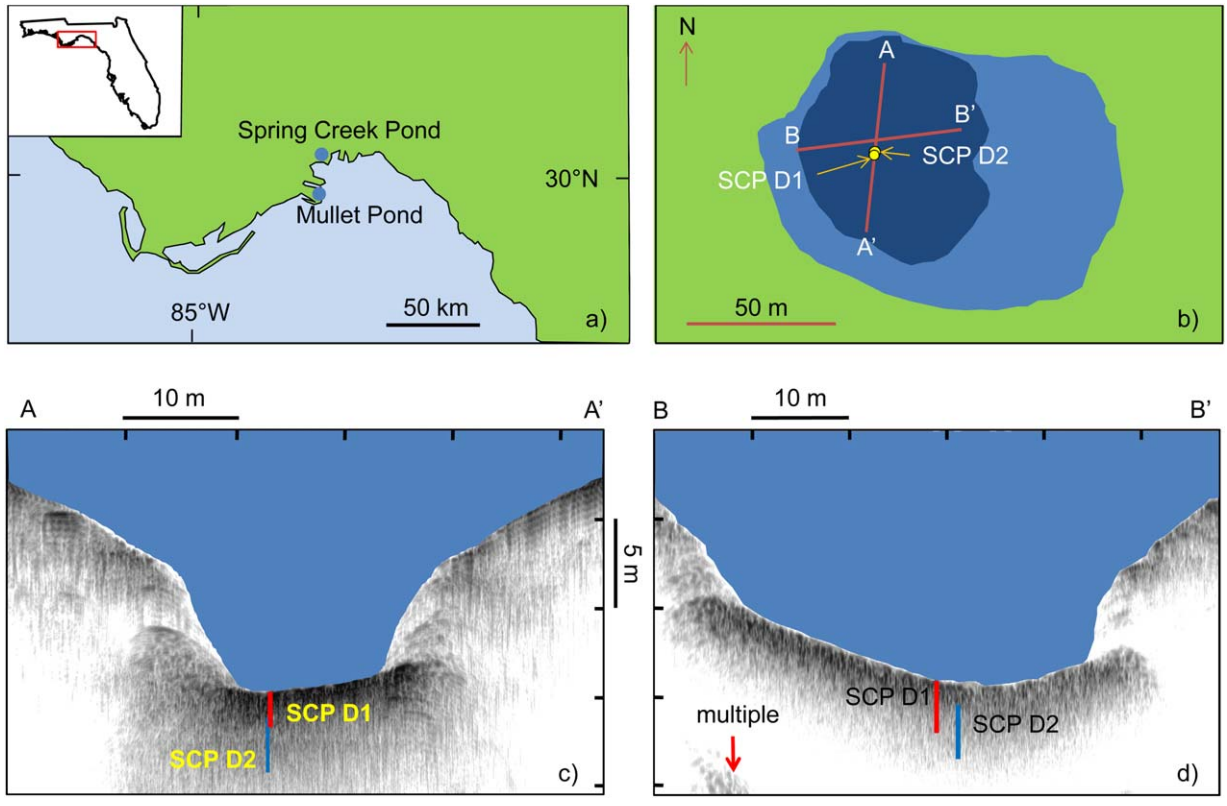

Figure 1. (a) Location of Spring Creek and Mullet Ponds on the coast of Apalachee Bay, Florida. Inset shows location of this area along Florida's coast. (b) Spring Creek Pond (light blue) and its sinkhole (dark blue). The two red lines correspond to sonar transects. Locations of cores SCP D1 and SCP D2 are shown. (c) Subbottom profile along line A-A′. Cores are shown at their proper location and depth. (d) Subbottom profile along transect B-B′. Cores are shown at their proper location and depth. "Multiple" refers to an instrument artifact and not a real subsurface feature.

of years. Sinkhole formation is an ongoing process and readily occurs in the saltwater/freshwater coastal mixing zone [*Randazzo and Jones*, 1997]. During the Miocene, another time when this area was submerged, quartz sands from the erosion of the Appalachian Mountains were overlain on the limestone bedrock [*Hine et al*., 1988]. Today, this sand is available for mobilization by hurricane storm surge and deposition in sinkhole ponds. Many of these ponds are deep and steep-sided thereby preventing remobilization of sediment after deposition.

[8] Mullet Pond, a sinkhole which was previously used in a paleotempest study [*Lane et al*., 2011], lies ~20 km to the south of SCP (Figure 1). The authors reconstructed a ~4500 year, decadally resolved, storm history of the area. This record was further analyzed for differences between "low-threshold" storm layers (i.e., the threshold above which most %coarse anomalies were identified as storm related) and "high-threshold" storm layers (storms which left deposits exceeding the highest %coarse anomaly left by a historic storm, in this case, Hurricane Elena in 1985 Common Era (C.E.)). Little variability was observed in low-threshold deposits at 95% confidence, but high-threshold deposits show periods of increased storm activity ~3800 calibrated years before present (B.P.) (~300 year period), ~3550 years B.P. (~100 year period), ~3300 years B.P. (~100 year period), 2800–2300 years B.P., 1200 years B.P. (50–100 year period), 900 years B.P. (~50 year period), 700 years B.P. (~100 year period) and decreased activity around 1800, 1650, 350, and 150 years B.P. This finding is somewhat different from earlier findings by *Liu and Fearn* [2000] for Western Lake located ~150 km to the west. Results from Western Lake show a drop in hurricane activity beginning ~1000 years ago [*Liu and Fearn*, 2000], but this could be related to coastal barrier dynamics changing the sensitivity of the site to overwash [*Otvos*, 2001]. Additional records

from the Apalachee region are nonetheless required to evaluate whether the patterns in overwash described by *Lane et al*. [2011] can be reproduced at nearby sites.

[9] Changes in relative sea level can greatly impact the occurrence of hurricane overwash at a site and therefore warrant consideration. Several studies have reconstructed sea-level curves for the Gulf of Mexico [*Stapor et al*., 1991; *Tanner*, 1992; *Morton et al*., 2000; *Törnqvist et al*., 2004; *Wright et al*., 2005; *Donnelly and Giosan*, 2008; *Milliken et al*., 2008]; however, there is some disagreement among these results. Some authors propose that sea level has continuously risen throughout the Holocene, with the rate of sea-level rise decreasing over time [*Otvos*, 2001; *Törnqvist et al*., 2004; *Wright et al*., 2005; *Donnelly and Giosan*, 2008; *Milliken et al*., 2008]. Others have proposed more complicated sea-level curves which include sea level "highstands" or periods of time when sea level was higher than it is today [*Stapor et al*., 1991; *Tanner*, 1992; *Morton et al*., 2000; *Blum et al*., 2002]. Proponents of mid-Holocene highstands use geomorphic observations and radiocarbon data from beach ridges to support the idea that these features were formed by wave deposition, and due to their heights, must have been formed at a time of higher-than-present sea level. *Donnelly and Giosan* [2008] offer an alternative explanation, that these ridges were formed during times of increased storm activity in the Gulf of Mexico, which increased the overall wave climate, leading to construction and preservation of these ridges. Further, *Lane et al*. [2011] found no indication of open marine sequences within the sediments and foraminifera assemblages at Mullet Pond, which refutes a mid-Holocene highstand in sea level. We rely on the sea-level rise data of *Wright et al*. [2005] and *Törnqvist et al*. [2006] which indicates a continuously, nearly linear rising sea-level rate of ~0.4 mm/yr for the region over the last ~3000 years.

3. Methods

3.1. Field Work

[10] Spring Creek Pond was visited during a field campaign in November 2011. The site was initially surveyed with a hand-held depth sounder and subbottom sonar profiles operating at 10 kHz (although the presence of gas resulted in limited subbottom sonar penetration within sediments). To preserve the sediment-water interface an initial 306 cm surface drive was obtained using a modified Vohnout/Colinvaux piston corer (i.e., SCP D1), following methods similar to *Donnelly and Woodruff* [2007]. Core SCP D1 was followed with a deeper piston vibracore (i.e., SCP D2) extending from 138 to 443 cm below the sediment-water interface. Both cores were obtained from approximately the center of the sinkhole (30°5.892′N, 84°19.681′W ± 3 m for SCP D1, and 30°5.891′, 84°19.681′W ± 3 m for SCP D2, Figure 1b). These cores were then shipped to the University of Massachusetts Amherst where they were split, described, and stored at 4°C refrigeration.

3.2. Analysis of Sediment Cores

[11] X-radiograph images of SCP D1 and SCP D2 split cores were taken with an Itrax Core Scanner (Cox Analytical) at UMass Amherst [*Croudace et al*., 2006]. The images have a resolution of 200 μm per pixel. The black and white inverted X-radiographs reveal density variations in the core with siliciclastic sand layers appearing much lighter than the surrounding silty, highly organic sediments (Figure 2a).

[12] Sediment cores were analyzed at 1 cm intervals for percent coarse (%coarse) material, corresponding to the silt-sand transition (e.g., >63 μm). These subsamples were sieved wet in order to prevent the aggregation of finer particles by drying, with the percent water (%water) obtained from a separate subsample. The %water was calculated by measuring the mass of the initial sample, drying it in an oven at 100°C for 24 h, and then weighing it again to obtain the dry mass. To determine the %coarse, another subsample was weighed wet with the separate %water measurements used to calculate the corresponding dry mass for the sample. Samples were then wet sieved at 63 μm with organics removed with 6% H_2O_2 at ~60°C prior to analysis. Sediments retained in the 63 μm sieve were then dried in an oven at 100°C for 24 h, and weighed to obtain the mass of coarse material and the corresponding %coarse relative to its calculated dry mass.

[13] The grain size distribution of the >63 μm portion of samples was obtained using a digital image processing, particle size and shape analyzer (Retsch Technology Camsizer), with distributions adjusted to account for %fines in each sample (i.e., <63 μm) lost through initial sieving. Grain size results are presented for D_{90}, which is defined as the size for which 90% of all other grain sizes in a distribution are smaller than.

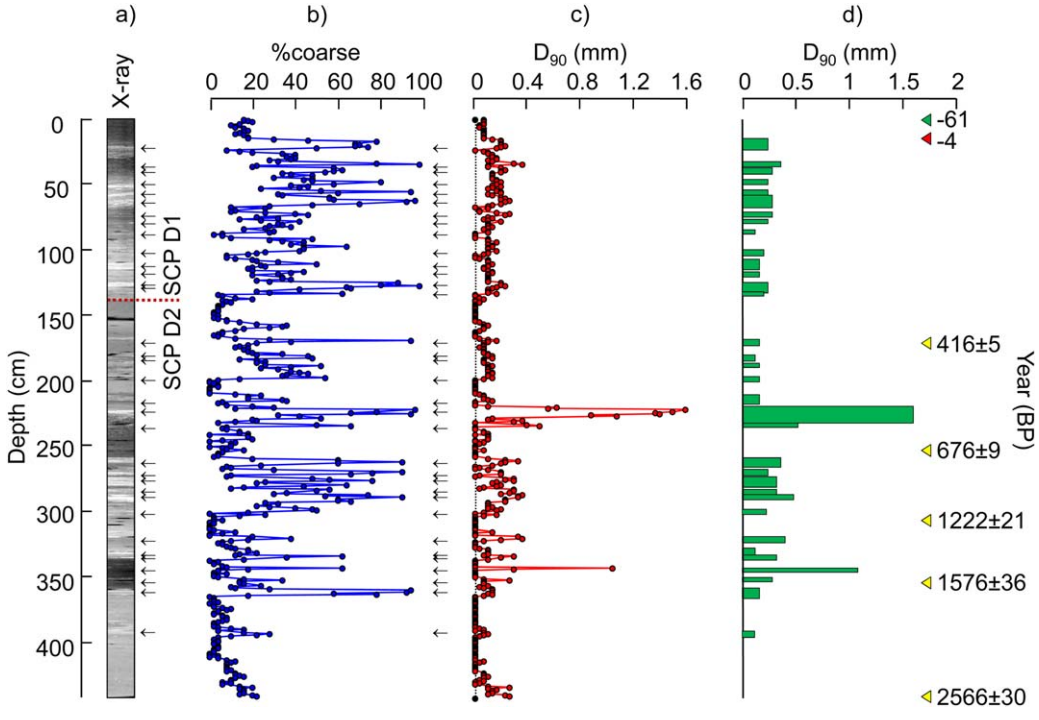

Figure 2. (a) Combined X-radiograph image of the SCP D1 and SCP D2 cores (separated by the dashed red line) extracted from Spring Creek Pond, showing density variations (lighter colors are denser). Arrows indicate inundation deposits. (b) Percentage of coarse material (grain size > 0.063 mm) sampled at 1 cm intervals. Peaks in %coarse (indicated with arrows) correlate with denser layers in X-radiograph. (c) Grain sizes at the 90th percentile (D_{90}), sampled at 1 cm intervals. The vertical dashed line at 0.063 mm indicates the silt-sand transition. (d) D_{90} grain size of the hurricane inundation layers. The vertical width of the bar is equal to the thickness of the deposit (as determined by the width of the D_{90} peak). ^{14}C data are shown with the yellow triangles, ^{137}Cs data with the red triangle, and the date of extraction (2011 C.E.) with the green triangle.

3.3. Radiometric Dating

[14] Cesium-137 (^{137}Cs) and lead-210 (^{210}Pb) were used to constrain modern deposition rates and the ages of historic storm deposits. The onset of ^{137}Cs in the sediment record is concurrent with the start of atmospheric nuclear weapons testing in 1954 C.E., with the peak in ^{137}Cs activity dating to 1963 C.E. [*Pennington et al*., 1973] just before the signing of the Nuclear Test Ban Treaty. ^{210}Pb ages were obtained using techniques similar to those described in *Woodruff et al*. [2012]. First, excess (unsupported) ^{210}Pb activity ($^{210}Pb_{ex}$) was obtained by subtracting the supported ^{210}Pb, as measured by the activity of ^{214}Pb [*Chen et al*., 2004] from the total ^{210}Pb activity. Next, a best-fit linear regression of the logarithm of ^{210}Pb excess versus the depth in the sediment was calculated [*Faure*, 1986; *Koide et al*., 1973; *Robbins and Edgington*, 1975], with the slope equal to the radioactive decay constant of ^{210}Pb (0.03114 yr^{-1}) divided by the average sedimentation rate. Discrete ages for individual ^{210}Pb measurements were obtained with the age-to-activity relationship described by *Appleby and Oldfield* [1978] when assuming a constant initial concentration of $^{210}Pb_{ex}$. Sediment samples were analyzed for ^{137}Cs and ^{210}Pb using a Canberra GL2020R Low Energy Germanium Detector at the University of Massachusetts Amherst. Each ~1.5–2.0 g dried sample was placed in a 6 cm diameter plastic jar and counted for 48–96 h. ^{137}Cs activities were computed spectroscopically using the 661.7 keV photopeak, ^{210}Pb activities were calculated using the 46.5 keV photopeak, and ^{214}Pb activities were obtained with the combined 74.8, 77.11, 87.3, 295.2, and 351.9 keV photopeaks.

[15] Carbon-14 (^{14}C) was used to date sediments older than the ^{210}Pb and ^{137}Cs derived age. Plant material at selected depths in the core was dated using Accelerator Mass Spectrometry (AMS) at the National Ocean Sciences Accelerator Mass Spectrometry Facility (NOSAMS) in Woods Hole, MA (Table 1). All radiocarbon ages were converted to years before present (B.P.) using IntCal09 [*Reimer*

et al., 2004], where "present" is defined as 1950 C.E. by convention. Anomalously old radiocarbon samples resulting in age reversals were excluded from the age chronology (see Table 1).

3.4. Numerical Modeling of Storm Inundation

[16] Numerical simulations were performed to constrain the range of hurricanes with the competence to transport the observed grain sizes into Spring Creek Pond under modern hurricane climatology. We then assume that this relationship provides a reasonable representation for the combination of storm characteristics (including wind speed, storm size, landfall location, intensity, forward translation speed, angle of approach, etc.), for hurricanes impacting the site prior to the instrumental record. To overcome restrictions associated with the limited number of historical overwash events affecting the site, we employed the model described by *Emanuel et al*. [2006], and hereafter referred to as the MIT model. The MIT model is a coupled ocean-atmosphere, beta and advection hurricane model that generates a database of tropical cyclones that pass a set distance from a site under modern climatic conditions. In the MIT model, a synthetic storm is created by first generating a storm track (the location of the storm's eye with a temporal resolution of 6 h) using a combination of historical storm track data and a synthetic wind field that conforms to monthly climatological means. Then, the storm's intensity is allowed to change based on a deterministic, coupled atmosphere-ocean model driven by shear derived from the synthetic wind field, monthly means of upper-ocean thermal structure, and potential intensity (the theoretical maximum intensity that a storm can achieve given certain environmental factors; see *Emanuel et al*. [2004]).

[17] The Sea, Lake, and Overland Surges from Hurricanes (SLOSH) model [*Jelesnianski et al*., 1992] was used with the Apalachicola (APC) grid to evaluate storm surge at the coast near Spring Creak Pond for each storm simulation from the MIT model. The National Weather Service SLOSH model simulates coastal inundation by solving differential equations (using finite-difference methods) which govern fluid motion. The hurricane, which is the driving force of the fluid motion, is modeled as a time-varying surface wind field and pressure gradient body force [*Jelesnianski et al*., 1992]. Of the 10,000 storms generated by the MIT model, 152 produced storm surges at the coastal grid cell closest to Spring Creek Pond that met or exceeded the 2.75 m elevation required to inundate the Spring Creek site. SLOSH simulations of time-varying water-level at this cell were extracted for each of these 152 storms.

Table 1. List of ^{14}C Ages

Sample	Depth in Core (cm)	Material	Mass (g)	Age ± Error (^{14}C year B.P.)	Calibrated Age (year B.P.)
1[a]	170	Bark	11.8	1300 ± 20	1270 ± 15
2[b]	172	Grass blade	3.6	240 ± 25	295 ± 10
3[c]	174.5	Leaf	1.3	95 ± 25	235 ± 15
4[a]	180	Bark	16.3	480 ± 25	520 ± 10
5[a]	209	Bark	3.3	390 ± 15	485 ± 15
6[a]	225	Bark	8.9	735 ± 25	675 ± 10
7	254	Bark	17.3	735 ± 25	675 ± 10
8	307	Bark	9.3	1260 ± 15	1220 ± 20
9	355	Twig	4.7	1680 ± 30	1575 ± 35
10	441.5	Bark	4.6	2500 ± 20	2565 ± 30

[a]Excluded from chronology due to anomalously old age.
[b]Used the oldest 2-σ age of 415 ± 5 years B.P.; see text for discussion.
[c]Age inconsistent with ^{210}Pb and ^{137}Cs chronology.

[18] Simulations of onshore inundation were performed using the Regional Ocean Modeling System (ROMS) [*Warner et al*., 2008] with a 2-D uniformly sloping grid and driven at its open boundary with water-level time series obtained from the 152 SLOSH simulations. ROMS is a numerical model that calculates the movement of water and sediment in various ocean and riverine environments [*Warner et al*., 2008]. It was used to model inundation at the Spring Creek site because it has a much finer horizontal resolution than the SLOSH model (10s of meters as opposed to 10s of kilometers for the SLOSH model) and is capable of resolving vertically varying flow fields, as well as resultant bottom shear stresses. While ROMS has the capability of creating a three-dimensional topography and bathymetry only a two-dimensional model was used here because of uncertainties associated with changing shoreline shape due to sea level rise over the course of the Holocene [*Stapor et al*., 1991; *Morton et al*., 2000; *Törnqvist et al*., 2004; *Wright et al*., 2005]. The coastline at the site is therefore not known over the later Holocene in the detail needed to warrant the use of a three-dimensional model.

[19] The landscape between the field site and the coast was modeled with a constant slope of 9.24×10^{-4} (as measured using USGS digital elevation models), and a constant quadratic drag coefficient of 0.0025. This drag coefficient was chosen from

the results of a ROMS model calibration using surge simulations produced by Hurricane Dennis in 2005 [see *Dukhovskoy and Morey*, 2011], and adjusted such that water levels reached, but did not exceed, Spring Creek Pond during the event (an observation consistent with first-hand accounts by local residents during the event). The ROMS model was given a horizontal resolution of 88 m and a vertical topographic resolution of 7.7 cm which were chosen as a balance between modeling speed and accuracy of results. The vertical resolution of the surge is variable such that there is higher resolution close to the bed and lower resolution closer to the water's surface [*Warner et al*., 2008]. Calculations were performed with a time step of 30 s with results saved at 20 min increments.

[20] Among its many outputs, ROMS calculates the bottom shear stress along the path of inundation at every time step. The maximum bottom shear stress at the grid cell corresponding to the field site was extracted and used in the Shields equation to calculate the competence for transport at the site:

$$\tau = \theta_c(\rho_s - \rho_w)gD_{90} \quad (1)$$

where τ is the bottom shear stress, θ_c is the nondimensional critical shields parameter, ρ_s is the density of the sediment (2650 kg/m^3 for quartz sand), ρ_w is the density of water (1000 kg/m^3), g is the acceleration due to gravity, and D_{90} is taken as the maximum grain size that can be mobilized by the flow [*Soulsby*, 1997]. Here, we use a value of 0.047 for θ_c [*Meyer-Peter and Müller*, 1948; *Julien and Wargadalam*, 1995; *Tjerry and Fredsøe*, 2005]. When combined, derived competence for transport for each of the 152 synthetic storms provides a relationship between the D_{90} grain size measured in deposits at SCP and the most likely hurricane intensity responsible for each deposit, with data dispersion constraining the uncertainty in this relationship.

[21] The distance between the coast and the site has likely decreased over the last few millennia as a result of sea-level rise. This leads to an increase in the sensitivity of the site to storm overwash and the maximum grain size advected to the site toward present. To account for these changes, the relationship between D_{90} grain size and wind speed is derived at the grid cell correlating to the elevation of the site above sea level at the time of deposition for each deposit within the Spring Creek Pond reconstruction. The data from *Wright et al*. [2005] and *Törnqvist et al*. [2006] were used to calculate a sea-level rise curve for this area, yielding an approximately linear rise of 0.4 mm/yr (Figure 3). Since the vertical topographic resolution is 7.7 cm, the virtual site was moved to the next up-slope grid cell every 7.7 cm/0.04 cm/yr = 192.5 years, which is equivalent to a sea-level fall from the present to the past.

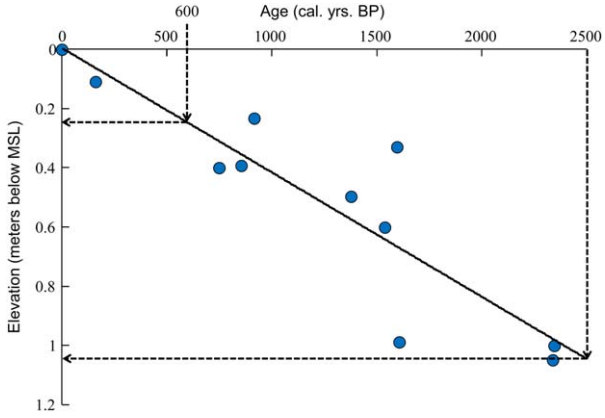

Figure 3. Sea level curve for the Gulf of Mexico using data from *Wright et al*. [2005] and *Törnqvist et al*. [2006]. A linear fit to the data (solid line) yields a sea level rise rate of 0.4 mm/yr. The sea level at 600 years B.P., corresponding to the deposition of the anomalous deposit, and 2500 years B.P., corresponding to the start of the Spring Creek record, are shown with the dashed lines.

4. Results

4.1. Sediment Chronology

[22] The age model for SCP D1 and SCP D2 is presented in Figure 4. The combined SCP record extends to a depth of 443 cm which corresponds to a maximum age of ~2580 years B.P. The ^{14}C data indicate that prior to ~600 years B.P., the sedimentation rate varied between 0.08 and 0.13 cm/yr. This rate increased to 0.31 cm/yr between ~600 and ~400 years B.P. and again to a rate of 0.38 cm/yr between ~400 and −4 year B.P. (1954 C.E.). The latter rate was calculated using the average age of the oldest 2-σ range (leftmost gray box in Figure 4) for the topmost ^{14}C date. If the average age had been used like in the previous calculations, then the deposition rates would be 0.18 cm/yr between ~600 and ~400 years B.P. and 0.63 cm/yr between ~400 and −4 years B.P., which are inconsistent with the deposition rates derived from the deeper radiocarbon dates as well as the historical deposition rates of 0.21–0.25 cm/yr based on ^{210}Pb derived chronologies and the 1954 C.E. onset of ^{137}Cs (Figure 4b). A 1963 C.E.

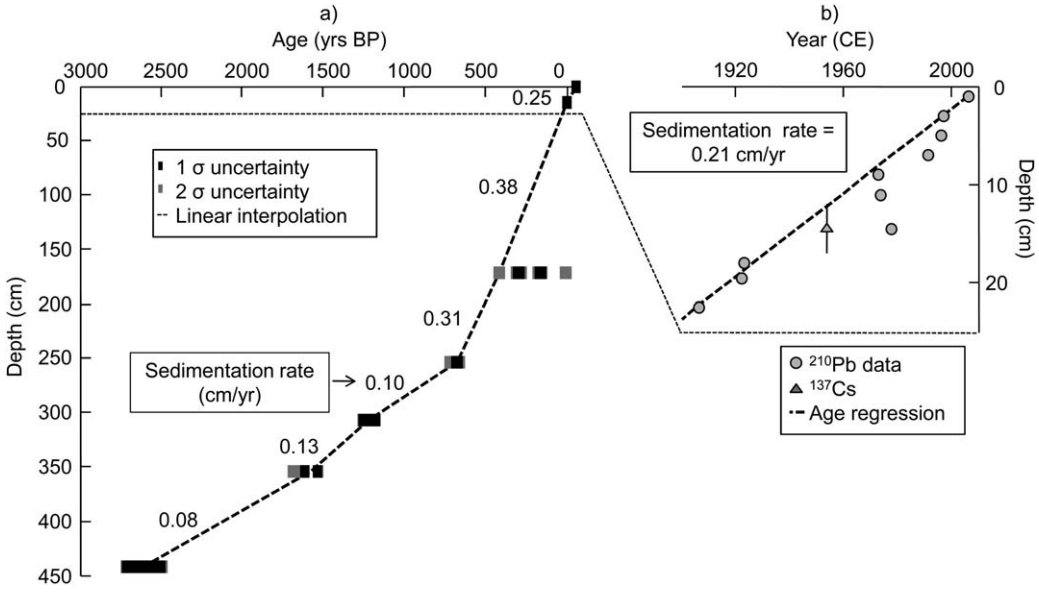

Figure 4. (a) Age model for SCP D1 and D2 using ^{14}C, ^{210}Pb, and ^{137}Cs data. 1-σ errors in the ^{14}C data are plotted as black boxes and 2-σ errors are plotted as gray boxes. The linearly interpolated sedimentation rate between each ^{14}C and ^{137}Cs data point is displayed. (b) A close-up of the ^{210}Pb and ^{137}Cs data. The 1-σ error in 1954 C.E. onset of ^{137}Cs due to the sampling interval is shown as a vertical line.

peak in ^{137}Cs was not observed within SCP, potentially due to the disruption of surficial sediments during extraction and transport.

4.2. Sedimentology

[23] Combined X-radiograph images and grain size data from SCP D1 and SCP D2 are presented in Figure 2, with Figure 5 showing data for the historic part of the sediment record. With few exceptions, significant peaks in %coarse correspond to peaks in D_{90} (Figures 2b and 2c) and light-colored (dense) deposits in the X-radiograph (Figure 2a), a finding consistent with past observations of hurricane-induced deposition within coastal marshes [e.g., *Boldt et al.*, 2010]. In total, 34 dense

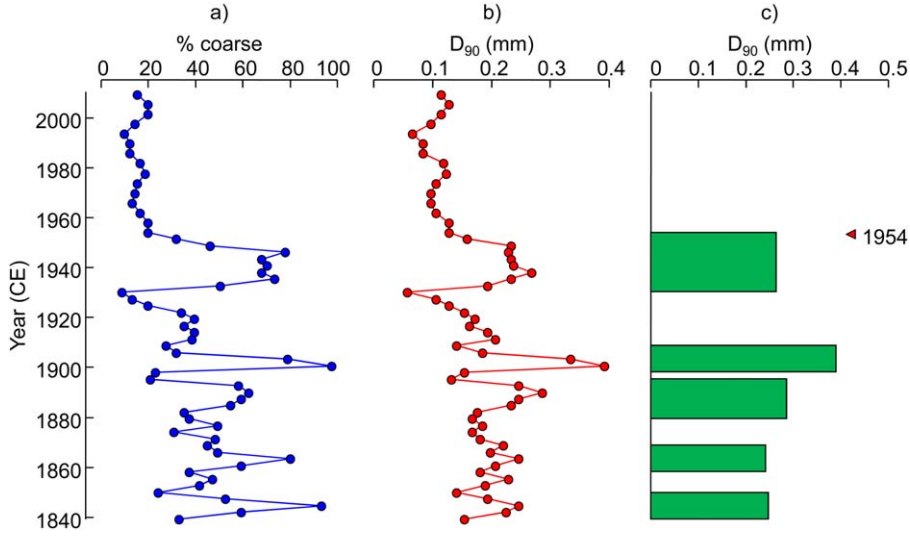

Figure 5. (a) %coarse (portion of material with diameters ≥0.063 mm) for the post-1840 C.E. portion of the sediment core. This age range is used to capture a storm whose temporal error bars put it within the historic period (post-1850 C.E.). (b) D_{90} grain size for the post-1840 C.E. portion. (c) D_{90} grain size for the inundation layers. The vertical height of the bar corresponds to the thickness of the deposit (measured using the width of the D_{90} spike). ^{137}Cs age constraint is shown with red triangle.

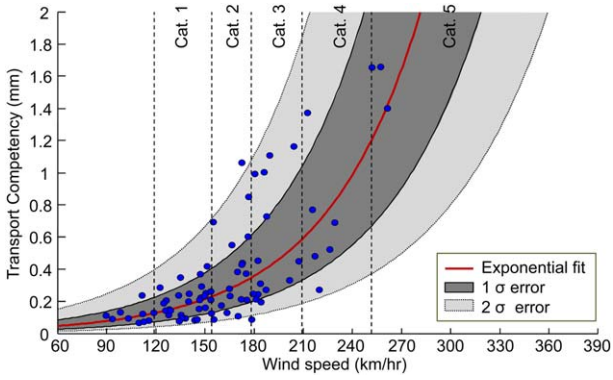

Figure 6. A plot of the surge competence and maximum landfall wind speed for each of the 80 storm surges (blue circles) which can transport a D_{90} grain size $\geq$0.063 cm. The red line is the exponential fit to the data. The dark gray area denotes the 1-σ error and the light gray area denotes the 2-σ error in the model. Vertical dashed lines indicate the boundaries of the wind speeds for each Saffir-Simpson hurricane category.

layers in the X-radiograph are delineated as event deposits based on corresponding peaks in %coarse and D_{90} grain size. Five of these deposits follow the 1851 C.E. onset of the best-track instrumental data set based on the core's derived ^{137}Cs, ^{14}C, and ^{210}Pb age model (Figure 4). *Lane et al*. [2011] also observed five deposits between 1845 and 1950 C.E. at Mullet Pond and correlated these to known hurricane landfalls in 1852, 1894, 1926, 1929, and 1941 C.E. Unfortunately, it is not known if these five deposits correspond to the five historical deposits seen in the Spring Creek record due to the temporal uncertainty of the emplacement of our deposits. An additional deposit was observed in the *Lane et al*. [2011] reconstruction following 1954 C.E. which potentially correlates to Hurricane Elena in 1985. This deposit is absent from the surficial sediments of the SCP core most likely due to disruption during transport of the core to UMass Amherst, as evidenced by a lack of the 1963 peak in ^{137}Cs in surficial SCP sediments.

[24] D_{90} grain sizes and %coarse for storm layers delineated at SCP range from 0.13 to 1.62 mm and 22–99%, respectively. Background (nonstorm layer) material has D_{90} grain sizes ranging from $<$0.063 mm (the grain size at which the samples were sieved for %coarse) to 0.207 mm and %coarse ranging from 0 to 37.0%. While most of the inundation layers have grain sizes ranging from very fine-grained to medium-grained sand, a particularly prominent layer, centered at 223.5 cm depth, has very coarse grains ($D_{90} = 1.62$ mm). A piece of a shell and some coral pieces were seen within this layer at 222.5 and 223.5 cm depth, supporting a marine origin.

4.3. Constraining Storm Wind Speed

[25] On the basis of bottom shear stresses derived from ROMS simulations for the 152 simulated storms with surge elevations $>$2.5 m at the coast, 80 are capable of transporting sand-sized ($\geq$0.063 mm) particles to Spring Creek Pond. Figure 6 plots the maximum wind speed at landfall for these 80 storms against the maximum grain size mobilized by each simulated event. When plotted together, the maximum wind speed (V_{max}) and surge grain size competence of transport (D) show an exponential relationship:

$$D = 10^{mV_{max}+b} \quad (2)$$

where m and b are the slope (0.01) and y-intercept ($-$1.8) of the linear regression of a log-log plot of the data, respectively.

[26] Error bars presented in Figure 6 point to the range of storm intensities capable of transporting sediments of a given grain size, with scatter in the data pointing to the other storm characteristics in addition to peak wind speed at landfall also influencing the magnitude of local flooding (e.g., landfall location in relation to the site, storm size, forward translation speed, and angle of approach). Despite these other factors, a majority of the variance in grain size for deposits at the site (72%) can be explained by the landfall wind speed alone.

[27] To assess the accuracy of the inverse model, we compare derived wind speeds for the five inundation deposits that occur during historic time to the measured landfall wind speeds of historic storms from the best-track data set. Modern storms considered to potentially affect the site are defined as those in the NOAA best-track data set [*Landsea et al*., 2004], which passed within 150 km of the site at hurricane strength (wind speeds $\geq$119 km/h or 74 mph). The timing and derived wind speeds for the inundation deposits falls within the range of measured landfall wind speeds for these historic hurricanes. Therefore, the model generally reproduces the intensities of historical hurricanes affecting the site, providing support for applying the technique to prehistoric deposits at Spring Creek Pond.

[28] In the Northern Hemisphere, the front right quadrant of a hurricane is often the most damaging because counter-clockwise rotational winds and

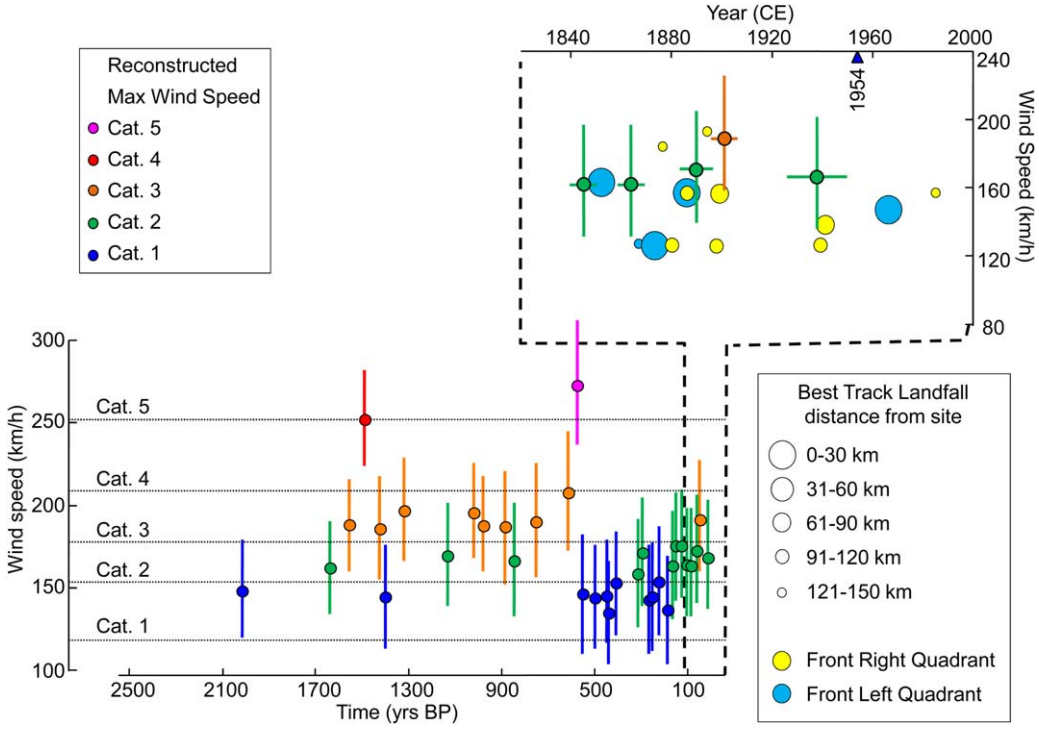

Figure 7. Time series of hurricane inundation events at Spring Creek Pond with calculated hurricane wind speeds and 1-σ error bars. Horizontal black lines indicate wind speeds denoting the Saffir-Simpson hurricane categories. Colors also correspond to Saffir-Simpson category: blue = category 1, green = category 2, orange-= category 3, red = category 4, and magenta = category 5. Inset: A comparison between storms from the best-track data set (blue and yellow circles) and the wind speed calculated from the five historic (post-1850 C.E.) inundation deposits in the Spring Creek Pond record (green and orange circles). Vertical error bars denote the 1-σ error in wind speed and horizontal bars denote error in dating of the deposit associated with sampling interval and thickness of deposit. The size of the circle of the best-track storms denotes the landfall distance from the site with larger circles corresponding to a smaller distance. Yellow circles are storms whose right-front (stronger) quadrant struck Spring Creek Pond and blue circles are storms whose left-front (weaker) quadrant struck the site. ^{137}Cs age constraint is shown with the blue triangle.

storm motion are in the same direction and combine to generate the greatest wind speeds. According to the NOAA best track data set [*Landsea et al*., 2004], 14 hurricanes passed within 150 km of the field site since 1851 C.E., five of which passed to the west (left) of SCP such that the most damaging front right quadrant of the storm impacted the site. Our sedimentary analysis also delineates five separate coarse deposits during this interval, a result similar to that from Mullet Pond by *Lane et al*. [2011]. However, as discussed previously, none of the deposits at SCP date to younger than 1954 C.E., which excludes one of the five hurricanes passing to the west of the site during the historical record. At least one of these event layers in SCP therefore reflects a hurricane passing to the east of SCP, such that the less severe front left quadrant impacted the site. Nonetheless, many of the more distal hurricanes that passed to the east of the site probably did not produce preserved deposits at SCP. This is likely one of the reasons our record does not capture all of the 14 historical hurricanes considered in Figure 7.

[29] Further, the time period between many of these 14 hurricanes is often shorter than the temporal resolution of our sampling. A modern sedimentation rate of 0.25 cm/yr for SCP results in a temporal resolution of 4 yr/cm. Of the 14 hurricanes to pass within 150 km of the SCP site 11 form four groups of storms too close together to be resolved individually within the SCP core (1873, 1877, and 1880; two storms in 1886; 1894, 1898, and 1899; 1939 and 1941), with storms in 1852 and 1966 passed to the east of SCP. Therefore, the five historical deposits observed at SCP generally correspond to the number of deposits we expected after accounting for limits associated with

temporal resolution and the intensity and landfall location of hurricanes impacting the site over the historical record.

4.4. Storm Frequency and Intensity

[30] The complete time series of inversely modeled wind speed for each coarse-grained deposit within the SCP reconstruction are presented in Figure 7. Model results indicate that all deposits observed at the Spring Creek Pond site are capable of being produced by storms with hurricane strength winds. One storm was detected between ~2500 and ~1700 years B.P. (0.1 storms/century), 14 storms between ~1700 and ~600 years B.P. (1.3 storms/century), and 19 storms between ~600 years B.P. and the present (3.2 storms/century). Nearly all of the major hurricanes (category 3 or greater) seen in this record occur during the period of activity from ~1700 to ~600 years B.P. (10 major hurricanes or 0.91 major hurricanes/century) and only one occurs post-600 years B.P. (0.17 major hurricanes/century).

[31] The uniqueness of an anomalously coarse layer at 220 cm or ~600 years B.P. (Figure 2) may indicate that it was formed by a process other than storm overwash. One possible origin of this unusually coarse deposit could be from a tsunami; however, this is unlikely due to the seismic stability of this area and its protection by Cuba and the Bahamas Platform from remotely generated tsunamis [*Randazzo and Jones*, 1997]. Another possible origin could be from heavy rainstorms transporting the surrounding sand into the pond. This scenario also seems unlikely since there is no evidence of surface flow to the pond and the surrounding low-relief landscape is well drained through the surficial Miocene sands underlain by fairly permeable limestone topography [*Puri and Vernon*, 1964; *Lane et al*., 2011]. Further, shells within the ~600 year B.P. layer point to a marine origin, while well-rounded sand grains in the deposit are indicative of beach material that has undergone some level of initial weathering by coastal processes. Additionally, inverse modeling results indicate that a hurricane of category 4 or 5 intensity is capable of producing the deposit. This result serves to highlight the significance of the exponential relationship between hurricane wind speed and competence of transport (i.e., Figure 6), with major hurricanes transporting grains of significantly greater sizes than less intense events. Wind speed estimates for the ~600 year B.P. event are 272 ± 40 km/h (169 ± 25 mph). This is far greater than the intensity for historical hurricanes affecting the site, however, Hurricane Camille (1969 C.E.) made landfall further to the east along the Gulf Coast of Mississippi with 306 km/h (190 mph) winds [Unisys, available from http://weather.unisys.com/hurricane/atlantic/1969/CAMILLE/track.dat], indicating that wind speed estimate for the 600 year B.P. event does fall within the range of known landfall wind speeds in the region.

5. Discussion

5.1. Clustering of Storms Toward the Present

[32] A notable increase in the frequency of lower intensity hurricane events is observed following ~600 years B.P., but the frequency of major hurricanes decreases during this same period. However, this increase in frequency is potentially an artifact due to (i) a change in sensitivity of the site to overwash due to rising sea level and (ii) greater undercounting of actual events prior to 600 years B.P. due to lower sedimentation rates. First, with rising sea level, the number of storms affecting the site should increase in recent centuries because the shoreline is moving closer to the site, decreasing the distance storm-induced floods must travel over land, as well as lowering the site's altitude above sea level. The sea level has risen ~1 m over the time span covered by this record (calculated using the sea level curve from *Donnelly and Giosan* [2008]), resulting in a lowering of the site from ~3.75 to 2.75 m above sea level. This has consequently caused the shoreline to move ~1 km closer to the site (calculated from USGS digital bathymetry maps) allowing storm surges to advect larger sediment grains to the site. Second, in addition to rising sea level leading to an actual increase in the number of storms affecting Spring Creek Pond, an increasing deposition rate can also lead to an apparent increase in their frequency due to biasing associated with under-counting events in sediments with significantly slower deposition rates [*Woodruff et al*., 2008a]. Figure 4 shows the ^{14}C, ^{210}Pb, and ^{137}Cs chronologies which reveal an increase in the deposition rate toward the modern age from an average of 1.0 mm/yr between ~2500 years B.P. and 600 years B.P. (calculated with the ^{14}C ages) to an average of 2.9 mm/yr between 600 years B.P. and the present (averaging the deposition rates from the ages of the youngest two ^{14}C samples, the 1954 C.E. onset of ^{137}Cs, and the ^{210}Pb chronology). This allows more storms to appear individually because there is less

time represented in each centimeter of sediment with many deposits older than 600 years B.P. possibly being amalgamations of two or more storms.

[33] An increase in sedimentation rate toward the present is common to lacustrine and lagoonal sediments along the Gulf of Mexico and the North Atlantic coasts due to increased connectivity of these systems to the sea as sea-level rises, resulting in an increase in the amount of marine sourced material introduced to these back-barrier environments [*Donnelly and Bertness*, 2001; *Donnelly et al*., 2004; *Gehrels et al*., 2005; *Woodruff et al*., 2008a]. Spring Creek Pond, however, is ~3 km inland and is not part of a coastal marsh system. Therefore, we do not believe that sea-level rise has contributed to the increased sedimentation rate at this site. Additional explanations include increased production from eutrophication and the compaction of older sediments. The underlying cause of the increased rate of sedimentation remains unclear. However, due to their concurrent timing, the increase in frequency of low-intensity hurricane events following 600 years B.P. is at least in part governed by the three-fold increase in sedimentation rate in the most recent centuries. It is possible that the frequency of low-intensity hurricane landfalls at the site has also increased over this time period; however, biasing associated with changes in sedimentation make it difficult to assess the significance of any potential changes in the frequency of lower-intensity events during this most recent interval.

5.2. Changes in Major Hurricane Frequency

[34] Changes in the landfall frequency of all hurricane categories are difficult to assess at SCP due to significant changes in rates of sedimentation. Trends in intensity for higher magnitude events, however, show additional patterns less affected by undercounting biases associated with changes in sedimentation rate. This is because, (i) these events occur less frequently and can be better resolved in a record of lower temporal resolution and (ii) more intense storms transport larger sediment grain sizes such that the maximum grain size within any deposit that is an amalgamation of several storms of different intensities will register as the most intense of these flood events.

[35] In the SCP reconstruction, the frequency of major hurricane strikes decreases from 0.91 storms/century between ~1700 and ~600 years B.P. to 0.17 storms/century between ~600 years B.P. and the present. This transition does not appear to be an artifact associated with an increase in sedimentation rate toward modern since the associated increase in temporal resolution should increase the number of deposits delineated in the record rather than decrease it. The drop in intense hurricane occurrences at 600 years B.P. is also inconsistent with increased sensitivity of the site to hurricane flooding from rising sea level. We therefore conclude that the decrease in the number of major hurricanes at ~600 years B.P. represents a real drop in the frequency of these more intense events at SCP.

5.3. Paleoclimate Comparisons

[36] The size of the SCP sinkhole is relatively small which limits the applicability for a transect of cores when compared to the larger back-barrier lagoons and marsh environments commonly used in other paleotempestological reconstructions. Alternatively, single core reconstructions from a series of nearby sinkholes provide a viable substitute to multicore analyses from a larger individual back-barrier marsh or lagoonal site. This study benefits from the nearby sinkhole reconstruction of hurricane overwash by *Lane et al*. [2011] at Mullet Pond, with comparisons to the SCP record helping to circumvent limitations associated with a reconstruction derived from a single core location at a single site. No significant trends were observed within the Mullet Pond reconstruction with respect to the frequency of all hurricanes; however, similar to the SCP reconstruction the Mullet Pond record exhibits a notable increase in the number of major hurricanes between 1500 and 600 years B.P. (with peak activity ~700 years B.P.), followed by a decrease in major hurricane activity between 600 years B.P. and present (Figures 8a and 8b). Trends in the SCP reconstruction therefore help to verify the initial findings of *Lane et al*. [2011] and provide further support for significant variability in the frequency of major hurricanes impacting Apalachee Bay over the last few millennia.

[37] Previous sedimentary reconstructions have related changes in hurricane activity to variations in North Atlantic sea surface temperatures (SSTs), the El Niño/Southern Oscillation (ENSO), and the North Atlantic Oscillation (NAO) [e.g., *Mann et al*., 2009; *Donnelly and Woodruff*, 2007; *Liu and Fearn*, 2000]. For instance, *Mann et al*. [2009] suggest that periods of more frequent hurricane landfalls in the last 1500 years correlate to times of warmer Atlantic SSTs and more La Niña-like

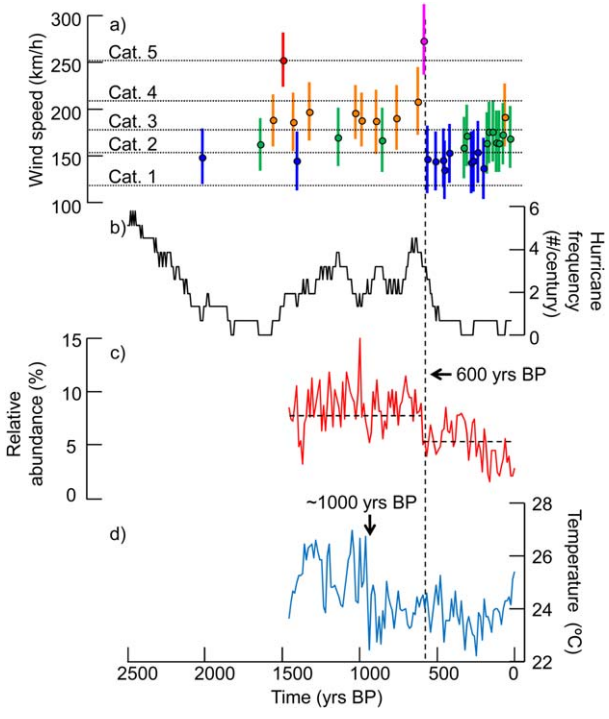

Figure 8. (a) Hurricane strike record at Spring Creek Pond spanning the past ~2500 years, compared to (b) the reconstructed frequency of intense hurricane events from the nearby site at Mullet Pond (MP) by *Lane et al*. [2011]. The color scheme in "a" is the same as in Figure 7 and the *y* axis of the MP record is intense (≥category 3) hurricane frequency (storms/century). (c) The relative abundance of *G. sacculifer* in the Pygmy Basin over the last ~1500 years. Increasing relative abundance of *G. sacculifer* corresponds to greater penetration of the Loop Current into the Gulf of Mexico. The horizontal dashed lines represent the mean value of *G. sacculifer* abundance, showing an abrupt decrease at 600 years B.P. (vertical dashed line), as presented by *Richey et al*. [2007]. (d) SST record, reconstructed from foraminiferal Mg/Ca ratios in the Pygmy Basin over the past ~1500 years [*Richey et al*., 2007]. The arrow indicates the drop in SST ~1000 years B.P. identified by the authors.

conditions. However, the active interval for intense hurricanes at Mullet and SCP ending at around 600 years B.P. is not predicted with the basin-wide statistical model of *Mann et al*. [2009]. This may indicate that variability in the Mullet Pond and SCP reconstructions represent changes more specific to the northeastern Gulf of Mexico, and in turn potentially forced by more regional forms of environmental change.

[38] Alternatively, discrepancies between the combined SCP/Mullet Pond reconstructions and the *Mann et al*. [2009] proxy record may indicate that other factors in addition to SST, ENSO, and the NAO are more dominant drivers of past changes in hurricane activity in the Gulf of Mexico. For instance, a better metric for the stability of the free troposphere, which in part governs the theoretical maximum wind speed that hurricanes can attain, is described by the difference between SST and temperature of the upper troposphere relative to SST rather than absolute SST alone [*Emanuel*, 1986, 1988]. Further, SST is often assumed to represent the temperature of the upper ocean mixed layer; however, this SST proxy provides very little information regarding the depth of the mixed layer, which in part determines how quickly cooler water from below can be mixed to the surface during the passage of a hurricane [*Emanuel et al*., 2004].

[39] It is possible that past variability in the position of the Loop Current in the Gulf of Mexico might explain regional changes in the frequency of intense hurricane landfalls represented by the SCP and Mullet Pond reconstructions [*Lane and Donnelly*, 2012]. The Loop Current is a surface-ocean current (part of the North Atlantic Western Boundary Current) that flows from the Caribbean Sea, northward through the Yucatan Channel into the Gulf of Mexico, loops to the east, and exits through the Florida Straits to join the Gulf Stream [*Poore et al*., 2003; *Lund and Curry*, 2004]. It is difficult to identify the Loop Current in the Gulf with SST alone; however, the importance of the Loop Current in controlling intense hurricane landfall frequency resides in how the current changes the Gulf's oceanic thermal structure rather than SST. In general, the mixed layer of ambient warm surface waters in the Gulf of Mexico has a relatively shallow average depth of 30–40 m [*Chouinard et al*., 1997]. As storms intensify, they quickly mix up cooler waters from below [*Price*, 1981; *Sriver and Huber*, 2007], and this process limits further storm development [*Emanuel et al*., 2004]. In the Loop Current, however, the mixed layer can be as deep as 200 m below the surface providing several times more available energy to developing cyclones by limiting the role of storm-induced upwelling [*Goni and Trinanes*, 2003].

[40] The deep, warm waters of the Loop Current occasionally meander northward into the eastern Gulf of Mexico and make a clockwise loop before exiting. These meanders periodically break off from the flow to form anticyclonic warm core eddies that propagate westward as they dissipate. The frequency of eddy formation and the extent to which the Loop Current penetrates into the Gulf is thought to be aperiodic on subdecadal time scales; however, lower-frequency variations in wind stress may drive periodicities on longer time scales

[*Sturges and Leben*, 2000]. The relative abundance of the foraminifer *Globigerinoides sacculifer* in marine cores taken from the Pigmy Basin in the northern Gulf has been offered as a proxy for the extent and/or frequency of Loop Current incursions into the Gulf [*Poore et al*., 2003, 2004, 2011*; Richey et al*., 2007]. Though not contemporaneous with regional SST cooling in Pigmy Basin at 1000 years B.P. as derived by Mg/Ca reconstructions, the significant decline in intense hurricane frequency occurring around 600 cal years B.P. at both SCP and Mullet Pond is concurrent with an abrupt decrease in *G. sacculifer* abundance at the Pigmy site [*Richey et al*., 2007]. The decline in *G. sacculifer* has been interpreted to reflect reduced advection of Caribbean surface waters into the Gulf of Mexico and a shoaling of the thermocline caused by a more southerly residence of the Loop Current [*Poore et al*., 2004]. A transition to less penetration of the Loop Current into the Gulf following 600 years B.P. would lower the ocean heat content available to tropical cyclones in the northeastern Gulf and might help to explain the 600 years B.P. drop in intense hurricane frequency observed both at SCP and Mullet Pond. Additional reconstructions are required, however, to confirm the hypothesized Loop Current proxy derived from Pigmy Basin.

6. Conclusions

[41] Sediments recovered from Spring Creek Pond, a coastal sinkhole located in northwest Florida, contain a ~2500 year record of hurricane activity in this area. We identify and date 34 storms layers and analyze each for %coarse material and D_{90} grain size. An inverse modeling technique is developed to constrain the landfall wind speed of the storms from the D_{90} grain size of their resultant deposits. We find that (1) applying the inverse model to the sediment deposits from the historic (post-1851 C.E.) record results in landfall wind speeds that are consistent with storms reported in the best-track data set, (2) all deposits throughout the ~2500 year record are capable of being produced by hurricanes, including a seemingly anomalous layer dated to 600 years B.P., and (3) the SCP time series of intense hurricane occurrence is consistent with a nearby reconstruction previously obtained from Mullet Pond, with both records indicating a period of increased intense hurricane frequency between ~1700 and ~600 years ago and decreased intense storm frequency from ~2500 to ~1700 and ~600 years ago to the present. The variation in intense hurricane strike frequency, particularly the drop in of activity at 600 years B.P., is potentially the result of inferred shifts in Loop Current penetration into the Gulf of Mexico.

Acknowledgments

[42] This work was supported by the National Science Foundation. We thank J. Elsner and J. Warner for valuable modeling assistance; K. Emanuel for sharing the data from the MIT model and his insightful comments and edits to an earlier version of the text; and S. Ahmed, A. Hawkes, D. MacDonald, S. Madsen, S. Moret, A. Sheldon, R. Sullivan, M. Toomey, P. van Hengstum, and S. Zipper for their field and laboratory assistance. This article benefited from constructive reviews by M. Huber, J. Anderson, and one anonymous reviewer.

References

Appleby, P. G., and F. Oldfield (1978), The calculation of lead-210 dates assuming a constant rate of supply of unsupported 210Pb to the sediment, *Catena*, *5*(1), 1–8, doi:10.1016/S0341–8162(78)80002-2.

Besonen, M. R., R. S. Bradley, M. Mudelsee, M. B. Abbott, and P. Francus (2008), A 1,000-year, annually-resolved record of hurricane activity from Boston, Massachusetts, *Geophys. Res. Lett.*, *35*, L14705, doi:10.1029/2008GL033950.

Blum, M. D., A. E. Carter, T. Zayac, and R. Gobel (2002), Middle Holocene sea-level and evolution of the Gulf of Mexico coast, *J. Coastal Res.*, *36*, 65–80.

Boldt, K. V., P. Lane, J. D. Woodruff, and J. P. Donnelly (2010), Calibrating a sedimentary record of overwash from Southeastern New England using modeled historic hurricane surges, *Mar. Geol.*, *275*(1–4), 127–139, doi:10.1016/j.margeo.2010.05.002.

Chen, Z., Y. Saito, Y. Kanai, T. Wei, L. Li, H. Yao, and Z. Wang (2004), Low concentration of heavy metals in the Yangtze estuarine sediments, China: A diluting setting, *Estuarine Coastal Shelf Sci.*, *60*(1), 91–100, doi:10.1016/j.ecss.2003.11.021.

Chouinard, L., C. Liu, and C. Cooper (1997), Model for severity of hurricanes in Gulf of Mexico, *J. Waterw. Port Coastal Ocean Eng.*, *123*, 120–129, doi:10.1061/(ASCE)0733–950X(1997)123:3(120).

Croudace, I. W., A. Rindby, and R. G. Rothwell (2006), ITRAX: Description and evaluation of a new multi-function X-ray core scanner, *Geol. Soc. Spec. Publ.*, *267*, 51–63.

Donnelly, J. P., and M. D. Bertness (2001), Rapid shoreward encroachment of salt marsh cordgrass in response to accelerated sea-level rise, *Proc. Natl. Acad. Sci. U. S. A.*, *98*(25), 14,218–14,223, doi:10.1073/pnas.251209298.

Donnelly, J. P., and L. Giosan (2008), Tempestuous highs and lows in the Gulf of Mexico, *Geology*, *36*(9), 751–752.

Donnelly, J. P., and J. D. Woodruff (2007), Intense hurricane activity over the past 5,000 years controlled by El Niño and the West African monsoon, *Nature*, *447*(7143), 465–468, doi:10.1038/nature05834.

Donnelly, J. P., S. S. Bryant, J. Butler, J. Dowling, L. Fan, N. Hausmann, P. Newby, B. Shuman, J. Stern, and K. Westover (2001a), 700 yr sedimentary record of intense hurricane

landfalls in southern New England, *Geol. Soc. Am. Bull.*, *113*(6), 714–727.

Donnelly, J. P., S. Roll, M. Wengren, J. Butler, R. Lederer, and T. Webb III (2001b), Sedimentary evidence of intense hurricane strikes from New Jersey, *Geology*, *29*(7), 615–618.

Donnelly, J. P., J. Butler, S. Roll, M. Wengren, and T. Webb (2004), A backbarrier overwash record of intense storms from Brigantine, New Jersey, *Mar. Geol.*, *210*(1), 107–121.

Dukhovskoy, D. S., and S. L. Morey (2011), Simulation of the hurricane Dennis storm surge and considerations for vertical resolution, *Nat. Hazards*, *58*(1), 511–540.

Elsner, J. B., T. H. Jagger, and K. Liu (2008), Comparison of hurricane return levels using historical and geological records, *J. Appl. Meteorol. Climatol.*, *47*(2), 368–374.

Emanuel, K. A. (1986), An air-sea interaction theory for tropical cyclones, Part I: Steady-state maintenance, *J. Atmos. Sci.*, *43*(6), 585–605, doi:http://dx.doi.org/10.1175/1520-0469(1986)043<0585:AASITF>2.0.CO;2.

Emanuel, K. A. (1988), The maximum intensity of hurricanes, *J. Atmos. Sci.*, *45*(7), 1143–1155.

Emanuel, K. A., C. DesAutels, C. Holloway, and R. Korty (2004), Environmental control of tropical cyclone intensity, *J. Atmos. Sci.*, *61*(7), 843–858.

Emanuel, K. A., S. Ravela, E. Vivant, and C. Risi (2006), A statistical deterministic approach to hurricane risk assessment, *Bull. Am. Meteorol. Soc.*, *87*(3), 299–314.

Faure, G. (1986), *Principles of Isotope Geology*, John Wiley, New York.

Frappier, A. B., D. Sahagian, S. J. Carpenter, L. A. González, and B. R. Frappier (2007), Stalagmite stable isotope record of recent tropical cyclone events, *Geology*, *35*(2), 111–114.

Gehrels, W. R., J. R. Kirby, A. Prokoph, R. M. Newnham, E. P. Achterberg, H. Evans, S. Black, and D. B. Scott (2005), Onset of recent rapid sea-level rise in the western Atlantic Ocean, *Quat. Sci. Rev.*, *24*(18), 2083–2100.

Goni, G., and J. Trinanes (2003), Ocean thermal structure monitoring could aid in the intensity forecast of tropical cyclones, *Eos Trans. AGU*, *84*(51), 573–580.

Hine, A. C., D. F. Belknap, J. G. Hutton, E. B. Osking, and M. W. Evans (1988), Recent geological history and modern sedimentary processes along an incipient, low-energy, epicontinental-sea coastline: Northwest Florida, *J. Sediment. Res.*, *58*(4), 567–579.

Jelesnianski, C. P., J. Chen, and W. A. Shaffer (1992), *SLOSH: Sea, Lake, and Overland Surges from Hurricanes*, U.S. Dep. of Commer., Natl. Oceanic and Atmos. Admin., Natl. Weather Serv., Silver Spring, Maryland.

Julien, P. Y., and J. Wargadalam (1995), Alluvial channel geometry: Theory and applications, *J. Hydraul. Eng.*, *121*(4), 312–325.

Koide, M., K. W. Bruland, and E. D. Goldberg (1973), Th-228/Th-232 and Pb-210 geochronologies in marine and lake sediments, *Geochim. Cosmochim. Acta*, *37*(5), 1171–1187.

Landsea, C. W., C. Anderson, N. Charles, G. Clark, J. Dunion, J. Fernandez-Partagas, P. Hungerford, C. Neumann, and M. Zimmer (2004), The Atlantic hurricane database re-analysis project: Documentation for the 1851–1910 alterations and additions to the HURDAT database, in *Hurricanes and Typhoons: Past, Present and Future*, edited by R. Murnane and K. Liu, pp. 177–221, Columbia Press, New York.

Lane, P., and J. P. Donnelly (2012), Hurricanes and typhoons: Will tropical cyclones become stronger and more frequent?, *PAGES Newslett.*, *20*(1), 32–33.

Lane, P., J. P. Donnelly, J. D. Woodruff, and A. D. Hawkes (2011), A decadally-resolved paleohurricane record archived in the late Holocene sediments of a Florida sinkhole, *Mar. Geol.*, *287*(1–4), 14–30.

Liu, K. B., and M. L. Fearn (1993), Lake-sediment record of late Holocene hurricane activities from coastal Alabama, *Geology*, *21*(9), 793–796.

Liu, K., and M. L. Fearn (2000), Reconstruction of prehistoric landfall frequencies of catastrophic hurricanes in northwestern Florida from lake sediment records, *Quat. Res.*, *54*(2), 238–245.

Lough, J. M. (2007), Tropical river flow and rainfall reconstructions from coral luminescence: Great Barrier Reef, Australia, *Paleoceanography*, *22*, PA2218, doi:10.1029/2006PA001377.

Lund, D. C., and W. B. Curry (2004), Late Holocene variability in Florida current surface density: Patterns and possible causes, *Paleoceanography*, *19*, PA4001, doi:10.1029/2004PA001008.

Malmquist, D. (1997), Oxygen isotopes in cave stalagmites as a proxy record of past tropical cyclone activity, in *22nd Conference on Hurricanes and Tropical Meteorology*, Am. Meteorol. Soc., Fort Collins, Colo.

Mann, M. E., J. D. Woodruff, J. P. Donnelly, and Z. Zhang (2009), Atlantic hurricanes and climate over the past 1,500 years, *Nature*, *460*(7257), 880–883.

Meyer-Peter, E., and R. Müller (1948), Formulas for bed-load transport, paper presented at the 2nd Meeting of the International Association for Hydraulic Structures Research, International Association of Hydraulic Research, Stockholm, Sweden, June 7, 1948.

Miller, D. L., C. I. Mora, H. D. Grissino-Mayer, C. J. Mock, M. E. Uhle, and Z. Sharp (2006), Tree-ring isotope records of tropical cyclone activity, *Proc. Natl. Acad. Sci. U. S. A.*, *103*(39), 14,294–14,297.

Milliken, K., J. B. Anderson, and A. B. Rodriguez (2008), A new composite Holocene sea-level curve for the northern Gulf of Mexico, response of Gulf coast estuaries to sea-level rise and climate change, *Geol. Soc. Am. Spec. Pap.*, *443*, 1–11.

Morton, R. A., J. G. Paine, and M. D. Blum (2000), Responses of stable bay-margin and barrier-island systems to Holocene sea-level highstands, western Gulf of Mexico, *J. Sediment. Res.*, *70*(3), 478–490.

Murnane, R. J. et al. (2000), Model estimates hurricane wind speed probabilities, *Eos Trans. AGU*, *81*(38), 433–438.

Noren, A. J., P. R. Bierman, E. J. Steig, A. Lini, and J. Southon (2002), Millennial-scale storminess variability in the northeastern United States during the Holocene epoch, *Nature*, *419*(6909), 821–824.

Nott, J. (2004), Paleotempestology: The study of prehistoric tropical cyclones—A review and implications for hazard assessment, *Environ. Int.*, *30*(3), 433–447.

Nyberg, J., B. A. Malmgren, A. Winter, M. R. Jury, K. H. Kilbourne, and T. M. Quinn (2007), Low Atlantic hurricane activity in the 1970s and 1980s compared to the past 270 years, *Nature*, *447*(7145), 698–701.

Otvos, E. G. (2001), Assumed Holocene highstands, Gulf of Mexico: Basic issues of sedimentary and landform criteria: Discussion, *J. Sediment. Res.*, *71*(4), 645–647.

Pennington, W., T. Tutin, R. Cambray, and E. Fisher (1973), Observations on lake sediments using fallout 137Cs as a tracer, *Nature*, *242*, 324–326, doi:10.1038/242324a0.

Peterson, L., J. Overpeck, N. Kipp, and J. Imbrie (1991), A high-resolution late quaternary upwelling record from the

anoxic Cariaco Basin, Venezuela, *Paleoceanography*, *6*(1), 99–119.

Poore, R., H. Dowsett, S. Verardo, and T. M. Quinn (2003), Millennial-to century-scale variability in Gulf of Mexico Holocene climate records, *Paleoceanography*, *18*(2), 1048, doi:10.1029/2002PA000868.

Poore, R., T. Quinn, and S. Verardo (2004), Century-scale movement of the Atlantic Intertropical Convergence Zone linked to solar variability, *Geophys. Res. Lett.*, *31*, L12214, doi:10.1029/2004GL019940.

Poore, R. Z., S. Verardo, J. Caplan, K. Pavich, and T. Quinn (2011), Planktic foraminiferal relative abundance and trends in Gulf of Mexico holocene sediments: Records of climate variability, in *Gulf of Mexico: Its Origins, Waters, Biota, and Human Impact, Geology*, vol. *3*, 1st ed., edited by Noreen A. Buster and C. W. Holmes, pp. 367–379, Texas A&M Univ. Press, College Station, Tex.

Price, J. F. (1981), Upper ocean response to a hurricane, *J. Phys. Oceanogr.*, *11*(2), 153–175, doi:http://dx.doi.org/10.1175/1520-0485(1981)011<0153:UORTAH>2.0.CO;2.

Puri, H. S., and R. O. Vernon (1964), *Summary of the Geology of Florida and a Guidebook to the Classic Exposures*, Special Publication No. 5, Fla. Geol. Surv., Tallahassee, Florida.

Randazzo, A. F., and D. S. Jones (1997), *The Geology of Florida*, 327 pp., Univ. Press of Fla., Gainesville, Fla.

Reimer, P. J. et al. (2004), IntCal04 terrestrial radiocarbon age calibration, 0–26 cal kyr BP, *Radiocarbon*, *46*(3), 1029–1058.

Richey, J. N., R. Z. Poore, B. P. Flower, and T. M. Quinn (2007), 1400 yr multiproxy record of climate variability from the northern Gulf of Mexico, *Geology*, *35*(5), 423–426.

Robbins, J. A., and D. N. Edgington (1975), Determination of recent sedimentation rates in Lake Michigan using Pb-210 and Cs-137, *Geochim. Cosmochim. Acta*, *39*(3), 285–304.

Scileppi, E., and J. P. Donnelly (2007), Sedimentary evidence of hurricane strikes in western Long Island, New York, *Geochem. Geophys. Geosyst.*, *8*, Q06011, doi:10.1029/2006GC001463.

Soulsby, R. (1997), *Dynamics of Marine Sands: A Manual for Practical Applications*, Thomas Telford, London.

Sriver, R. L., and M. Huber (2007), Observational evidence for an ocean heat pump induced by tropical cylones, *Nature*, *447*, 577–580, doi:10.1038/nature05785.

Stapor, F. W., Jr., T. D. Mathews, and F. E. Lindfors-Kearns (1991), Barrier-island progradation and Holocene sea-level history in southwest Florida, *J. Coastal Res.*, *7*(3), 815–838.

Sturges, W., and R. Leben (2000), Frequency of ring separations from the Loop Current in the Gulf of Mexico: A revised estimate, *J. Phys. Oceanogr.*, *30*(7), 1814–1819, doi:http://dx.doi.org/10.1175/1520-0485(2000)030<1814:FORSFT>2.0.CO;2.

Tanner, W. F. (1992), 3000 years of sea level change, *Bull. Am. Meteorol. Soc.*, *73*(3), 297–303.

Tjerry, S., and J. Fredsøe (2005), Calculation of dune morphology, *J. Geophys. Res.*, *110*, F04013, doi:10.1029/2004JF000171.

Törnqvist, T. E., J. L. González, L. A. Newsom, K. van der Borg, A. F. de Jong, and C. W. Kurnik (2004), Deciphering Holocene sea-level history on the US Gulf Coast: A high-resolution record from the Mississippi Delta, *Geol. Soc. Am. Bull.*, *116*(7–8), 1026–1039.

Törnqvist, T. E., S. J. Bick, K. van der Borg, and A. F. de Jong (2006), How stable is the Mississippi Delta?, *Geology*, *34*(8), 697–700.

USEPA (1999), Ecological condition of estuaries in the Gulf of Mexico, Rep. EPA 620-R- 98-004, pp. 80, U.S. Environmental Protection Agency, Office of Research and Development, National Health and Environmental Effects Research Laboratory, Gulf Ecology Division, Gulf Breeze, Florida.

Wallace, D. J., and J. B. Anderson (2010), Evidence of similar probablility of intense hurricane strikes for the Gulf of Mexico over the late Holocene, *Geology*, *38*(6), 511–514.

Warner, J. C., C. R. Sherwood, R. P. Signell, C. K. Harris, and H. G. Arango (2008), Development of a three-dimensional, regional, coupled wave, current, and sediment-transport model, *Comput. Geosci.*, *34*(10), 1284–1306.

Woodruff, J. D., J. P. Donnelly, K. Emanuel, and P. Lane (2008a), Assessing sedimentary records of paleohurricane activity using modeled hurricane climatology, *Geochem. Geophys. Geosyst.*, *9*, Q09V10, doi:10.1029/2008GC002043.

Woodruff, J. D., J. P. Donnelly, D. Mohrig, and W. R. Geyer (2008b), Reconstructing relative flooding intensities responsible for hurricane-induced deposits from Laguna Playa Grande, Vieques, Puerto Rico, *Geology*, *36*(5), 391–394.

Woodruff, J. D., A. Martini, E. Elzidani, T. Naugton, D. Kekacs, and D. G. MacDonald (2012), Off-river waterbodies on tidal rivers: Human impact on rates of infilling and the accumulation of pollutants, *Geomorphology*, *184*, 38–50.

Wright, E. E., A. C. Hine, S. L. Goodbred, and S. D. Locker (2005), The effect of sea-level and climate change on the development of a mixed siliciclastic–carbonate, deltaic coastline: Suwannee River, Florida, USA, *J. Sediment. Res.*, *75*(4), 621–635.